ARTICLE

A rapid and simple electrochemical detection of the free drug concentration in human serum using boron-doped diamond electrodes

Received 00th January 20xx,
Accepted 00th January 20xx

DOI: 10.1039/x0xx00000x

Hideto Moriyama,[‡a] Genki Ogata,[‡a] Haruma Nashimoto[b], Seishiro Sawamura[c], Yoshiaki Furukawa[a], Hiroshi Hibino[c], Hiroyuki Kusuhara[b] and Yasuaki Einaga*[a]

Monitoring drug concentration in the blood and reflecting this in the dosage is crucial for safe and effective drug treatment. Most drug assays are based on total concentrations of bound and unbound protein in the serum, although only the unbound concentration causes beneficial and adverse events. Monitoring the unbound concentration alone is expected to provide a means for further optimisation of drug treatment. However, unbound concentration monitoring has not been routinely used for drug treatment due to the long analysis time and the high cost of conventional methods. Here, we have developed a rapid electrochemical method to determine the unbound concentration in ultrafiltered human serum using boron-doped diamond (BDD) electrodes. When the anticancer drug doxorubicin was used as the test drug, the catalytic doxorubicin-mediated reduction of dissolved oxygen provided a sensitive electrochemical signal, with a detection limit of 0.14 nM. Contrarily, the sensitivity of glassy carbon (GC) was inferior under the same conditions due to interference from the dissolved oxygen reduction current. The signal background ratio (S/B) of BDD and GC was 11.5 (10 nM of doxorubicin) and 1.1 (50 nM), respectively. The results show that a fast measurement time within ten seconds is possible in the clinical concentration range. Additionally, in the ultrafiltered human serum, the obtained values of unbound doxorubicin concentration showed good agreement with those quantified by conventional liquid chromatography-mass spectrometry. This approach has the potential for application in clinical settings where rapid and simple analysis methods would be beneficial.

Introduction

Drugs administered into the human body are absorbed into the bloodstream and distributed throughout the body by blood circulation. Drug molecules are present as protein-bound and free forms in the blood and tissues. The protein-bound form is a complex of drug and serum proteins such as albumin and α1-acid glycoprotein, formed by reversible binding to the pocket of the proteins via van der Waals and hydrogen bonds due to hydrophobic and electrostatic interactions.[1] According to Free Drug Theory, only the unbound form of a drug is available to interact with proteins. Thus, their concentration is essential for the exposure-response analysis of drugs. Generally, the unbound fraction, a ratio of the concentration of unbound to the total, is used to estimate the concentrations of unbound form in the blood/plasma under the assumption that a dissociation equilibrium is established.

The composition of blood protein varies depending on age and physical constitution. In the literature, it was observed that when a patient developed hypoalbuminemia or other such conditions, the unbound drug concentration differed considerably compared to a healthy person.[2,3] Therefore, the measurement of unbound drug concentrations is helpful to maximise the efficacy of drug treatment while minimising side effects for patients. However, the unbound drug concentrations in the blood have not been routinely monitored in clinical settings and reflected in drug treatment. This situation is since unbound drug concentration monitoring has conventionally been performed by conventional instrumental analysis methods such as liquid chromatography-mass spectrometry (LC-MS, LC-MS/MS), liquid high-performance chromatography-ultraviolet detection (HPLC-UV), and liquid scintillation counter (LSC),[4,5] following ultrafiltration or equilibrium dialysis to separate the unbound form. Although these are highly accurate and sensitive methods to measure the available unbound
ion in the blood, they have a long measurement time, a
ibitive cost, a large instrument size, and require
olicated procedures. These conventional methods are not
ble for drug therapy monitoring for patients who need
results in a clinical environment.
n response, we propose a simple and highly sensitive
rochemical measurement as an alternative to the
entional approach to determine the unbound drug
entration. Electrochemical measurements are generally

[a] Department of Chemistry, Keio University, 3–14–1 Hiyoshi, Yokohama 223–8522, Japan. E-mail: einaga@chem.keio.ac.jp
[b] Laboratory of Molecular Pharmacokinetics, Graduate School of Pharmaceutical Sciences, The University of Tokyo, 7-3-1 Hongo, Bunkyo, Tokyo 113-0033, Japan
[c] Division of Glocal Pharmacology, Department of Pharmacology, Graduate School of Medicine, Osaka University, 2-2 Yamadaoka, Suita, Osaka 565-0871, Japan
†Electronic Supplementary Information (ESI) available: [Figure S1–S9, and Table S1–S3]. See DOI: 10.1039/x0xx00000x. ‡Contributed equally.

faster than instrumental methods due to the speed of electron transfer that occurs between the electrode and the reactant. They also have advantages over conventional methods in terms of cost and the measurement environment can be easily miniaturised. Hence, an electrochemical method is expected to be more applicable to measure the unbound drug concentration in real clinical settings.

Whilst electrodes of various materials have been used for electrochemical measurements, a novel boron-doped diamond electrode (BDD) was used in this study. Diamond is an insulator, but when doped with boron, it becomes conductive and can be used as an electrode material. BDD has outstanding properties as an electrode material, such as good physical and chemical stability, low background currents, a wide potential window in aqueous solutions, resistance to physical and chemical adsorption, and biocompatibility.6-8 Furthermore, a significant advantage of BDD is that it offers sustainable and repeatable measurements. A simple application of potential can easily clean the surface of the BDD electrode because the BDD does not become damaged even when a high potential such as ±3.0 V *vs*. Ag/AgCl is applied. In contrast, a glassy carbon electrode surface cannot be effectively cleaned by simply applying electrical potentials because the electrode surface becomes damaged by high potentials. Polishing operations are required for every measurement when using glassy carbon. Because of these excellent features, BDD is a suitable electrode material for drug measurement in a biological environment.

We selected doxorubicin as the target drug for measuring the unbound concentration in this study because this drug can be measured at a nanomolar level using BDD electrodes.[9] Doxorubicin is one of the anthracycline antibiotics and a widely used anticancer drug for treatment. Several mechanisms of its action interfere with the replication of cancer cells, for example, by intercalating with DNA base pairs and disrupting the topoisomerase-II-mediated DNA repair.[10,11] Although this drug is effective against various cancers, it has cardiotoxicity as a primary side effect. Therefore, careful control is needed when administering the drug.[10,11]

In this work, firstly, we have evaluated the fundamental electrochemical reaction of doxorubicin on the BDD surface and examined its mechanism. Subsequently, the unbound drug concentration of doxorubicin in human serum was measured using BDD electrodes. All the samples of the unbound drug were prepared by ultrafiltration using Centrifree®. The same samples used for the BDD measurements were also quantified using LC-MS/SM for comparison. The measured concentrations using both methods were in good agreement. These results demonstrate that our approach provides a fast and straightforward unbound doxorubicin concentration measurement. We show that this approach has allowed us to quantify the unbound concentration of doxorubicin in human serum over a range of clinically relevant concentrations.

Experimental section

Chemicals

Doxorubicin hydrochloride was purchased from LKT Laboratories, Inc., and the other reagents were purchased from FUJIFILM Wako Pure Chemical Corporation and used without any purification. Doxorubicin hydrochloride was dissolved in dimethyl sulfoxide (DMSO) for long-term storage without any purification. The stock solution (100 μM) was stored at room temperature (25 ℃) with light shielding. The phosphate buffer (PB, 0.1 M) consisted of NaH_2PO_4 and $Na_2HPO_4{\cdot}12H_2O$, and the acetate buffer (0.1 M) consisted of CH_3COOH and CH_3COONa. After adjusting the pH, PB, the acetate buffer, and a KCl-HCl buffer (0.1 M) were used as the electrolyte. Sulfuric acid (H_2SO_4; 0.1 M) was used for cleaning the BDD by cathodic reduction. All the solutions were prepared with pure water supplied from DIRECT-Q 3 UV (Merck Millipore Corporation) with a specific resistivity of 18.2 MΩ·cm. Pooled human serum was purchased from Kohjin Bio Co., Ltd. and stored frozen at −20 ℃. Before use, it was thawed to room temperature.

Preparation of the BDD electrodes

The method used for preparing the BDD electrodes was similar to that used in our previous studies.[12] The BDD electrodes were prepared using a microwave plasma-assisted chemical vapour deposition (CVD) system (Model AX5250M, ASTex, Inc.). A mixture of acetone and trimethoxyborane ($B(OCH_3)_3$) was used as the carbon (C) and boron (B) source at a B/C ratio of 1%. The BDD films were deposited on silicon wafers with plasma power for six hours. The film quality was confirmed by Raman spectroscopy (Acton SP2500, Princeton Instruments). Measurements were performed at 9 locations on the BDD electrode and the obtained Raman spectra were analysed. Raman spectroscopy showed typical spectra with a peak at 1,300 cm^{-1}, denoting sp^3 carbon bonds (Figure S1). Both peaks observed at around 500 and 1,200 cm^{-1} confirm the existence of boron doping in the diamond structure, whilst no peak was observed at approximately 1,600 cm^{-1}, which would generally be attributed to sp^2 carbon (Figure S1†). These observations indicate that the BDD was of superior quality.[13,14] In addition, the surface morphology and crystalline structure of the BDDs were examined with a field emission scanning electron microscope (SEM, accelerating voltage: 15 kV, JCM-6000Plus, JEOL Co.). The images showed that all the films were polycrystalline and uniformly coated on the substrate, with no visible cracks, pinholes, or voids (Figure S2†).[12] The polycrystalline diamond with a grain size was approximately 5 μm.[12] Furthermore, the quality of the BDD was confirmed by cyclic voltammetry in 0.1 M PB (pH 7.4) (Figure S3†).

Preparation of human serum samples

Thawed human serum was transferred to a low protein adsorption tube (PROTEOSAVE® SS 15 mL Conicaltube, Sumitomo Bakelite Co.). The doxorubicin stock solution (50, 100 μM) in DMSO was added to the serum and stirred well. The amount of DMSO to serum was adjusted to be less than 1% for preventing protein denaturation by DMSO. An aliquot of 1 mL sample serum was transferred to a Centrifree® Centrifugal Filter Device (Amicon Bioseparations, Millipore) and placed in the incubator at 37.5 ℃ for 30 minutes. The samples were then

centrifuged at 1100 g for 10 minutes at room temperature in a Hitachi Koki Model CF16RX Ⅱ (Hitachi Koki Co., Ltd.). The filtrate was collected and divided into two sample groups. Samples of one group were diluted 6-fold by adding PB (pH 6.0) and used for electrochemical measurements using the BDD electrode. The other samples were diluted 4-fold by adding acetonitrile and centrifuged (5000 rpm, 5 min, 25 °C) for precipitating and removing the proteins from the serum filtrated samples. These treated samples were used for the LC-MS/MS measurements to compare the values obtained from both methods.

Electrochemical measurement

All the measurements were performed at room temperature in a Faraday cage. Measurements were conducted in a standard three-electrode system in a Teflon cell with BDD and glassy carbon (GC) as the working electrode. At the same time, a Pt wire and Ag/AgCl (saturated KCl) were used as the counter and reference electrodes, respectively (Figure S4†). The working electrode was mounted on the bottom of the cell using a silicon O-ring (JIS standard, P-7) and connected to a potentiostat (Autolab, PGSTAT204, Metrohm Inc.) through a Cu plate placed under the working electrode. The area of the working electrode was estimated to be 0.312 cm^2. Before use, the BDD and Pt wire was pretreated by ultrasonication in 2-propanol and pure water for 10 minutes, respectively. The silicon O-ring was pretreated by ultrasonication in ultrapure water also for 10 minutes. To prepare the hydrogen-terminated BDD, a cathodic reduction at −3.0 V *vs*. Ag/AgCl in 0.1 M aqueous sulfuric acid for 10 minutes by chronoamperometry (CA) was performed. Before each measurement, ultrasonication in 0.5 M aqueous sodium hydroxide for 3 minutes and cathodic reduction at −3.0 V vs. Ag/AgCl for 5 minutes was performed, respectively. The GC electrode was polished with alumina powder for 10 minutes and we confirmed that the surface became clean and mirror-like before each measurement. All the electrochemical measurements were performed by linear sweep voltammetry (LSV).

LC-MS/MS measurement

The solutions subjected to the assessment of the LC-MS/MS measurements were as follows. First, an aliquot of 5 µL of the stock solutions of doxorubicin (0, 2, 4, 8, 16, and 32 µM in DMSO) was diluted with 395 µL of ultrafiltered serum solution (see Preparation of human serum samples in Methods). Then, a 4-fold volume (1600 µL) of acetonitrile was added into the ultrafiltered serum solution with doxorubicin and centrifuged for 5 min at 5000 rpm (room temperature, Hitachi Koki Model CF16RX Ⅱ (Hitachi Koki Co., Ltd.)) to remove residual proteins. The supernatants were used for calibration standard (CS) samples of the drug at 0, 5, 10, 20, 40, and 80 nM (1000 µL for each). As well as these CS solutions, also used as the quality control (QC) samples were 5, 20, and 80 nM solutions, which denoted references for low, mid, and high concentrations, respectively. The preparation of spiked human serum test samples is described above (see Preparation of human serum samples in the Methods). For each sample, the injection volume into the LC-MS/MS was 10 µL.

The LC was operated in a UFLC Prominence HPLC (Shimadzu Co., Japan) using the Atlantis® T3 column (2.1 mm × 50 mm, 3 µm, Waters Co., USA) at 40 ºC with a flow rate of 0.4 mL min−1. The mobile phase consisted of A: ultra-pure water and B: acetonitrile. The chromatography schedule commenced with 20% of A in B for 10 min. The MS/MS was performed using electrospray ionisation using a LCMS-8050 triple quadrupole mass spectrometer (Shimadzu Co., Japan). Mass spectrometric settings were optimised to obtain the maximum signal for each of the selected reaction monitoring transitions; the determined parameters are provided in Table S1†. The quantitative analysis of doxorubicin was conducted in positive mode using a multiple reaction monitoring method. In this context, the quantification was attributed to selected reaction monitoring using the m/z 544.20→m/z 397.05 transition for doxorubicin.

The LC-MS/MS data were acquired and analysed by LabSolutions ver.5.82 (Shimadzu Co.). The calibration curve was obtained by plotting the peak area in the CS samples (Figure S5 and S6†). The curves were fitted using a least-squares linear regression method. The lower limit of quantification of doxorubicin was 0.188 nM (Figure S6†). The mass spectrometric signals obtained from the ultrafiltered human serum samples with doxorubicin were converted to the diluted concentration using the calibration curves. Then the obtained values were multiplied by 5 to get the actual unbound concentration.

Data analysis

Igor Pro (WaveMetrics Inc.) and Microsoft Excel were used to analyse the data obtained from all measurements. GraphPad Prism9 (GraphPad Software Inc.) was used for determining regression. The mean ± standard error of the mean (s.e.m.) was used as descriptive statistics. The standard deviation (SD) of the background signal and the slope of the calibration curve were used to calculate the limit of detection (LOD) by following equations (1).

$$LOD = 3\,SD/slope \qquad (1)$$

Results and discussion

Electrochemical reduction of doxorubicin

Linear sweep voltammetry (LSV) of 0.1 M PB (pH 7.4) and with 10 nM doxorubicin using the BDD electrode were performed (Figure 1a). In the presence of doxorubicin, a large voltammetric peak was observed at -0.55 V (*vs*. Ag/AgCl). The broad peak at −0.92 V obtained in both cases is expected to be due to the reduction of dissolved oxygen.[15,16]

We also measured doxorubicin using a glassy carbon electrode, a common electrode material made of carbon in the same way as BDD. The reduction peak of doxorubicin was not observed using the GC electrode, even in 50 nM doxorubicin (Figure 1b). The background current of GC is larger than the BDD background current and thus, the oxygen reduction peak overlaps the peak of doxorubicin (Figure S7†). On the contrary, the BDD electrode has minimal background current and the

oxygen reduction peak at around −1.0 V(Figure 1a and S7†). Therefore, a clear peak was obtained even in a small concentration of 10 nM with BDD. In addition, the signal background ratio (S/B) of BDD and GC was 11.5 (10 nM of doxorubicin) and 1.1 (50 nM), respectively. Therefore, BDD has significant advantages over GC in terms of high sensitivity

We also investigated the mechanism of the electrochemical reduction of doxorubicin. We measured the LSV of doxorubicin in 0.1 M PB (pH 7.4) and 0.1 M KCl-HCl buffer (pH 1.0) for evaluating the influence of pH in the electrochemical reaction (Figure 2). At a pH of 1.0, the reduction peak of doxorubicin was not obtained at a concentration of 10 nM. At a concentration of 10000 nM (10 mM), a small peak current around −0.2 V was obtained (Figure 2, blue line). These results suggest that the reduction pathway of doxorubicin is different depending on the pH.

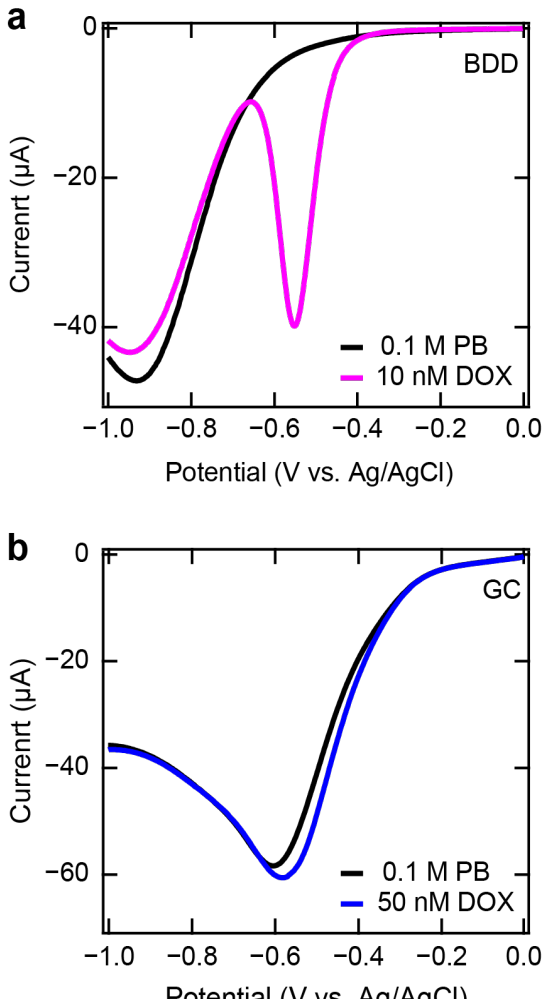

Figure 1. Linear sweep voltammograms of doxorubicin in 0.1 M PB (pH 7.4). (a) BDD, in the absence (black line) and the presence of 10 nM doxorubicin (DOX, magenta line). (b) GC, in the absence (black line) and the presence of 50 nM doxorubicin (DOX, blue line).

Next, we discuss the reaction of the doxorubicin depending on the pH. The benzoquinone moiety of doxorubicin is known to be reduced to hydroquinone by a two-electron/two-proton

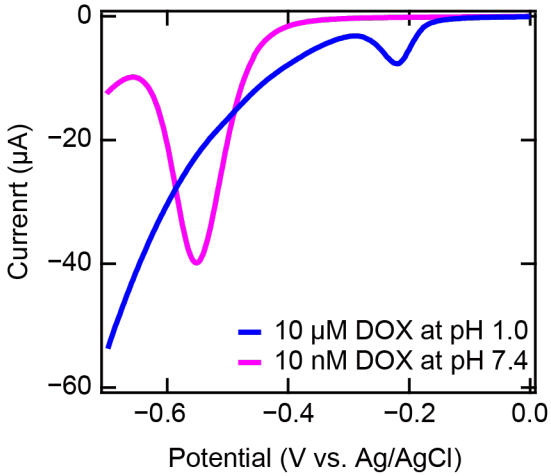

Figure 2. Linear sweep voltammograms of doxorubicin in different pH. The magenta line shows 10 nM doxorubicin (DOX) in 0.1 M PB at pH 7.4, and the blue line shows 10000 nM (10 μM) doxorubicin (DOX) in 0.1 M KCl-HCl buffer at pH 1.0. Start potential: 0 V vs. Ag/AgCl; Scan rate: 100 mV s^{-1}.

redu
anthi
on the solution pH.[19-21] Figure 4 shows the reduction pathway of anthraquinone. AQ and AQH_2 represent anthraquinone and anthrahydroquinone, respectively. At a pH 4-7, anthraquinone is reduced to anthrahydroquinone with an electron transfer (E)–chemical reaction (C)–electron transfer–chemical reaction (ECEC) mechanism in which the process of electron transfer followed by a chemical reaction occurs twice. However, an EECC process mainly occurs around pH 11, and the reduction pathway follows the alternative CCEE mechanism at low pH (around pH 1). The pKa of reaction intermediates explains the difference in reaction pathways.[21]

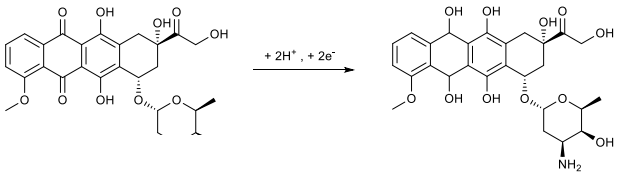

Figure 3. Electrochemical reduction of doxorubicin.[17,18]

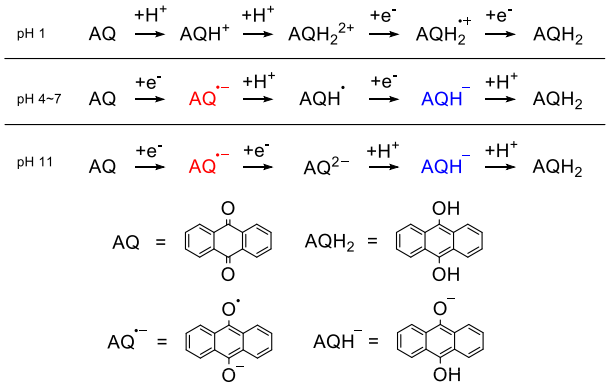

Figure 4. Reduction pathway of anthraquinone at each pH.[19-21] AQ and AQH_2 represent anthraquinone and anthrahydroquinone, respectively.

Furthermore, an essential factor in reducing anthraquinones is the side reaction with dissolved oxygen. Li et al. state[20] that some reaction intermediates are active against oxygen and cause feedforward loop reactions, as shown in Figure 5.

$$AQ^{\bullet -} + O_2 \rightleftharpoons AQ + O_2^{\bullet -}$$
$$AQH^{-} + O_2 \rightleftharpoons AQ + HO_2^{-}$$

Figure 5. The reaction of semiquinone ions with oxygen.[20]

The semiquinone ions, $AQ^{\bullet -}$ and AQH^{-} react with oxygen to produce reactive oxygen species (ROS). Thereby the semiquinone ions revert to anthraquinones. Figure 4 shows that the two reaction intermediates ($AQ^{\bullet -}$ and AQH^{-}) are present in the reduction pathways at pH values of 4~7 and 11. On the contrary, neither intermediate is present in the reduction pathway at pH 1, suggesting oxygen is not involved in the reaction at this pH. Thus, we considered that at a pH of 7.4, the two-electron/two-proton reduction of the benzoquinone moiety and the reaction of the intermediate with oxygen to revert to the original doxorubicin molecule occur simultaneously. These phenomena cause the catalytic cycle and the increased number of reaction electrons to generate a considerable current value (Figure 2, red line). Conversely, at a pH 1.0, no intermediate reacts with oxygen in the reaction pathway as described above. Therefore, only a two-electron/two-proton reduction occurs, and the current value is smaller than that of pH 7.4 (Figure 2, blue line). These results suggest that dissolved oxygen has an essential role in reducing doxorubicin. Accordingly, we measured LSV in the solution after degassing oxygen by nitrogen bubbling (Figure 6). The peak current was 70.0 µA without N_2 bubbling (Figure 6, magenta line), 16.9 µA with 1 min bubbling (Figure 6, blue line), and 13.3 µA with 10 min bubbling (Figure 6, green line). The peak current values decreased with an increasing nitrogen bubbling time. This result indicates that dissolved oxygen is deeply involved in the electrochemical reduction of doxorubicin.

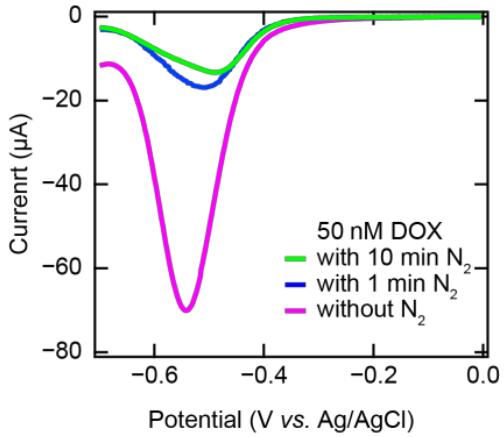

Figure 6. Linear sweep voltammograms of 50 nM doxorubicin in 0.1 M PB (pH 7.4). The magenta line shows the voltammogram of 50 nM doxorubicin (DOX) without N_2 bubbling, the blue line with 1 min N_2 bubbling, and the green line with 10 min N_2 bubbling. Start potential: 0 V vs. Ag/AgCl; Scan rate: 100 mV s^{-1}.

Investigation of concentration dependence

Figure 7 shows calibration curves in the range of 0-100 nM doxorubicin. The measurements were performed in PB solutions (pH 7.4, 6.0) and acetate buffer (pH 5.1) by using LSV. The voltammograms of LSV measurements are shown in Figure S8[+]. A linear calibration curve in the range of 0-100 nM was obtained at pH 5.1(Figure 7a red line, slope = 0.1777, R^2 = 0.9959, LOD = 5.90 nM). At pH 6.0 and 7.4, the calibration curves were fitted the non-linear with good fits of X^2 (Figure 7a blue line, R^2 = 0.9989) and ln(X) (Figure 7a green line, R^2 = 0.9748), respectively. At these three pHs, the reduction of doxorubicin has been shown to follow the same pathway (Figure 4). However, these measurements revealed that the reactivity differs depending on the solution pH, even in this range.

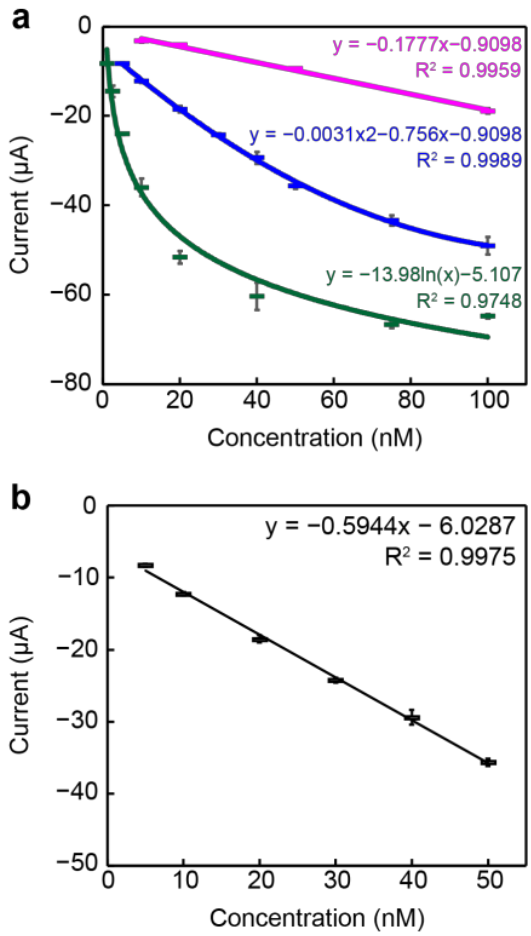

Figure 7. Calibration curves of doxorubicin at each pH. (a) Magenta line and bars indicate caliburation line and data obtained at pH 5.1 (10, 20, 50, 100 nM in 0.1 M acetate buffer, n = 3); blue line and bars: at pH 6.0 (5, 10, 20, 30, 40, 50, 75, 100 nM doxorubicin in 0.1 M PB, n = 5); green line and bars: at pH 7.4 (1, 2.5, 5, 10, 20, 40, 75, 100 nM doxorubicin in 0.1 M PB, n = 3). (b) Calibration curve at pH 6.0 (range: 5-50 nM). Data are shown in mean ± s.e.m.

The LOD of doxorubicin at pH 7.4 was estimated to be 0.14 nM. Under this condition, quantification at low concentration was achieved. On the other hand, the current value increase became slower at high concentrations, and no concentration-

dependent increase of the current value was observed above 80 nM. This phenomenon was considered due to the limited amount of dissolved oxygen that reacts with the intermediates of doxorubicin. Comparable results have been reported in the measurement of quinizarin, which is the moiety of doxorubicin.[22] At a weakly acidic pH, although the detection and quantification limits are higher than at a pH 7.4, this has the advantage that higher concentrations can be measured. These results suggest that measuring a wide concentration range is possible by adjusting the solution pH.

At a pH 6.0, a linear calibration curve was obtained in a concentration range of 5-50 nM (Figure 7b, slope: 0.5944, R^2 = 0.9975, LOD = 1.63 nM). However, when the concentration exceeded 75 nM, the current value gradually reached a plateau value. According to the literature, when patients were given a dose of 75 mg/m^2 by intravenous drip for 15 min, the plasma concentration of doxorubicin decreases from about 5 mM to 100 nM within one hour, and the concentration falls to about 10 nM after 96 hours administration.[23] The LOD obtained in this study (1.63 nM) is well below these concentrations. Furthermore, photodegradation of doxorubicin in phosphate buffer solutions around pH 7 was reported.[24-26] In contrast, the doxorubicin was sufficiently stable for over 12 hours at around pH 6.[27] For these reasons, we chose pH 6.0 as a condition for the following measurements.

Measurement of unbound concentration in human serum.

Samples were prepared by spiking doxorubicin (DMSO stock solution) into the human serum with a concentration of 500 nM (Entry 1,3,4) and 1000 nM (Entry 2,5,6). These samples were ultrafiltered and prepared for BDD and LC-MS/MS measurements (see Preparation of human serum samples in the Methods). For the LSV measurement, we diluted filtrate samples 6-fold by adding PB (pH 6.0). The reasons for this dilution were the following. The clinical plasma concentrations from 30 min to 96 hours after administration of doxorubicin were reported to be about 10 to 300 nM.[23] Thus, we set the measuring concentration range between 10 to 300 nM. A linear calibration curve was obtained within the 5-50 nM concentration range at a pH 6.0 (Figure 7b). Therefore, we could quantify up to 300 nM by diluting the sample 6-fold. In addition, 10 nM samples did not fall below the LOD of 1.63 nM, even with 6-fold dilution.

Table 1 The calculated serum concentration of unbound doxorubicin.

Entry	Electrode	Unbound concentration (nM)	
		BDD	LC-MS/MS
1	BDD-A	62.52	73.47
2	BDD-A	147.45	187.37
3	BDD-B	104.19	107.09
4	BDD-B	86.20	95.24
5	BDD-B	143.57	150.86
6	BDD-B	127.80	138.61

We used two different BDD (electrodes A and B) to verify the reproducibility between the electrodes in the LSV measurements (Figure 8). The obtained current values were converted to the unbound concentration of doxorubicin (Table 1) using calibration curves prepared before measurement (Figure S9†). The reproducibility of each electrode was verified to calculate the coefficients of variation (CV) using the calibration data (n = 3, Figure S9†). CV values using BDD-A and BDD-B were 1.3-9.9% and 2.4-11.9%, respectively (Table S2). CV≤15% is generally accepted as a bioanalytical assay[28,29]. Our results of CV value were lower than 15%.

Furthermore, we quantified the same samples using the LC-MS/MS to evaluate the concentration obtained using the BDD (Table 1).

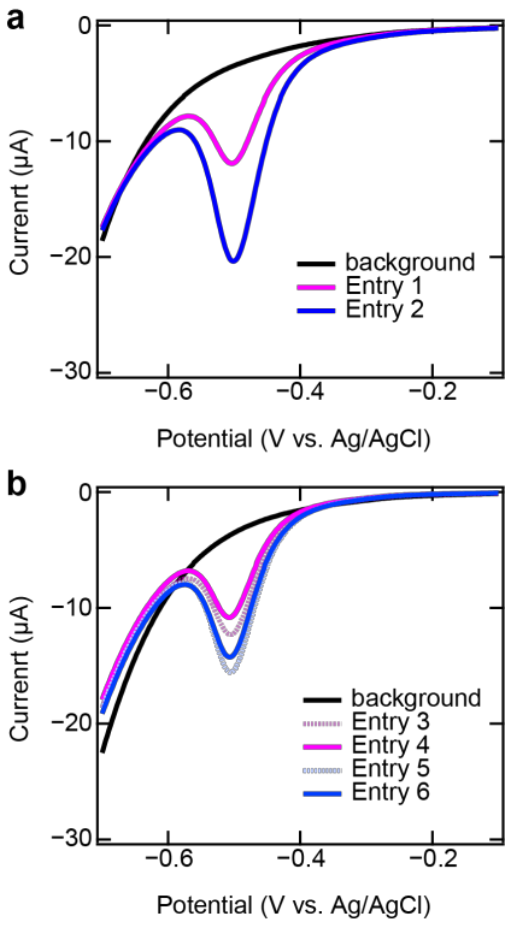

Figure 8. Linear sweep voltammograms of unbound doxorubicin at pH 6.0. (a) shows measurements using BDD-A, and (b) shows using BDD-B. Start potential: 0 V vs. Ag/AgCl; Scan rate: 100 mV s^{-1}.

The calculated serum concentrations of doxorubicin shown in Table 1 were plotted with the BDD results on the horizontal axis and the LC-MS/MS results on the vertical axis (Figure 9). Then, the Deming regression was applied for evaluating the degree of agreement between both methods. The slope of Deming regression was 1.242 and was not statistically different from 1.0 (P-value = 0.300). These results suggest that the electrochemical measurements using BDD have a good agreement with those from the LC-MS/MS method.

Furthermore, Table 2 shows the percentage of unbound fraction (F_u%) in human serum calculated from the measurements of each sample. When the concentration of

doxorubicin in human serum was 500 nM, the average F_u% was 16.9 ± 2.41% (mean ± s.e.m.), and when 1000 nM, it was 14.0 ± 0.60% (mean ± s.e.m.). These results agree with the values of previous studies (15-33%),[23,30,31] indicating that our method effectively measures the unbound drug concentration in human serum.

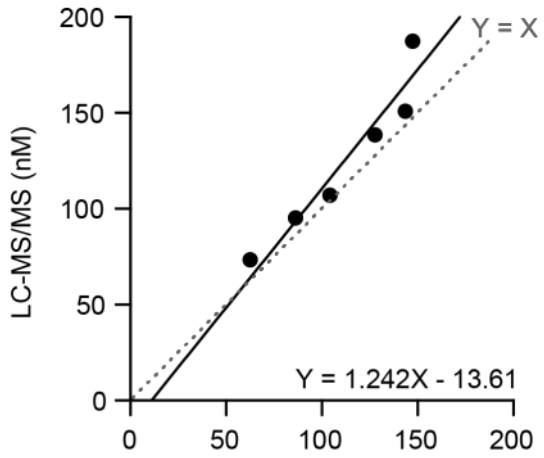

Figure 9. Comparison of BDD and LC-MS/MS method by Deming regression. The solid line indicates the Deming regression line from the results of this work. The dashed grey line indicates Y = X.

Table 2. Percentage of unbound concentration calculated from the measurements by BDD.

Entry	Concentration Add (nM)	Unbound C* (nM)	Fu# (%)
1	500	62.5	12.5
2	1000	148	14.7
3	500	104	20.8
4	500	86.2	17.2
5	1000	144	14.4
6	1000	128	12.8

*: Unbound C means unbound concentration. #: Fu means the unbound fraction, a ratio of the concentration of unbound to the total

Many doxorubicin sensors have been developed[32]. We summarised the comparisons between these sensors and the BDD electrode in Table S3. According to this comparison, we found several advantages of our study. (i) For a limit of detection (LOD), this study obtained better results than most other works. (ii) While most other electrodes require complex surface preparation and modification, BDD can be easily prepared by chemical vapour deposition (CVD) and can be used without surface modification. (iii) BDD can be used repetitively with simple electrochemical pretreatment.

Hence, these results suggest that the electrochemical measurement using BDD can measure unbound drug concentrations as effectively as LC-MS/MS. This study indicates that our strategy is effective as a rapid and straightforward method for measuring unbound drug concentration in medical settings. Further development of medicine could be expected from fast and straightforward drug monitoring using electrochemical techniques using BDD electrodes in the future.

Conclusion

In the present work, the measurement of the unbound concentration of doxorubicin in human serum was achieved in the clinical concentration range by means of an electrochemical measurement using boron-doped diamond electrodes. Firstly, the reduction mechanism of doxorubicin was investigated by basic electrochemical measurements. There was a noteworthy difference in the reactivity of doxorubicin between pH 1.0 and pH 7.4, which showed the same tendency as the reaction of anthraquinone, the moiety of doxorubicin. We have demonstrated that oxygen is crucial for the doxorubicin reduction from a decrease in the peak current after degassing oxygen with nitrogen bubbling. The quantification of doxorubicin was achieved at three different pH values (pH 5.1, 6.0, 7.4). The measurement concentration range was controlled by adjusting the solution pH according to the purpose. The unbound doxorubicin concentration in human serum was measured using simple centrifugation and electrochemical measurement. The obtained results agreed with the conventional LC-MS/MS results. Our procedure does not require expert knowledge or skills, and the equipment is relatively inexpensive and compact compared to LC-MS/MS. Since the measurement time is shorter than conventional methods, the method has broad applicability to clinical situations. Using BDD electrodes, the electrochemical measurement of personal unbound drug concentrations in patients could become more accessible.

Conflicts of interest

The authors declare no competing financial interests.

Author Contributions

‡H.M. and G.O. contributed equally to this work. H.M., G.O., H.N., S.S., Y.F., H.H., H.K., and Y.E. designed the experiments. H.M., G.O., and H.N. developed the experimental setup. H.M., G.O., and Y.E. prepared the BDD electrodes. H.N. and H.K. contributed to establishing the protocol for the LC-MS/MS experiments. H.M., G.O., and Y.E. performed the electrochemical experiments. H.M. and G.O. designed and performed the LC-MS/MS experiments. H.M., G.O., H.N., S.S., Y.F., H.H., H.K., and Y.E. analysed the results. H.M., G.O., and Y.E. authored the paper. All authors edited the paper.

Acknowledgements

This study was partially supported by the following research grants: Grant-in-Aid for Challenging Exploratory Research 20K21883 (to H.H.); Grant-in-Aid for Scientific Research A

18H04062 (to H.H.); AMED-CREST (Grant Number: 21gm1510004) (to H.H.); Grant-in-Aid for Scientific Research A 19H00832 (to Y.E.); Grant-in-Aid for Scientific Research B 18H03513 (to G.O.); Grant-in-Aid for Scientific Research B 21H03805 (to G.O.); Grant-in-Aid for Young Scientists 20K16005 (to S.S.), Fukuda Foundation for Medical Technology (to G.O.); and Yamaguchi Educational and Scholarship Foundation (to G.O.).

References

1 T. Ghafourian and Z. Amin, *BioImpacts*, 2013, **3**, 21–27.
2 R. Gugler, D. W. Shoeman, D. H. Huffman, J. B. Cohlmia and D. L. Azarnoff, *Journal of Clinical Investigation*, 1975, **55**, 1182–1189.
3 Boston Collaborative Drug Surveillance Program, *Clin Pharmacol Ther*, 1973, **14**, 529–532.
4 S. M. Illamola, D. Hirt, J. M. Tréluyer, S. Urien and S. Benaboud, *Drug Discov Today*, 2015, **20**, 466–474.
5 B. Seyfinejad, S. A. Ozkan and A. Jouyban, *Talanta*, 2021, **225**, 122052.
6 J. H. T. Luong, K. B. Male and J. D. Glennon, *Analyst*, 2009, **134**, 1965–1979.
7 Y. Einaga, *Bull Chem Soc Jpn*, 2018, **91**, 1752–1762.
8 J. V. Macpherson, *Physical Chemistry Chemical Physics*, 2015, **17**, 2935–2949.
9 G. Ogata, Y. Ishii, K. Asai, Y. Sano, F. Nin, T. Yoshida, T. Higuchi, S. Sawamura, T. Ota, K. Hori, K. Maeda, S. Komune, K. Doi, M. Takai, I. Findlay, H. Kusuhara, Y. Einaga and H. Hibino, *Nat Biomed Eng*, 2017, **1**, 654–666.
10 C. F. Thorn, C. Oshiro, S. Marsh, T. Hernandez-Boussard, H. McLeod, T. E. Klein and R. B. Altman, *Pharmacogenet Genomics*, 2011, **21**, 440–446.
11 P. A. Henriksen, *Heart*, 2018, **104**, 971–977.
12 A. Fujishima, Y. Einaga, T. N. Rao and D. A.Tryk, *Diamond Electrochemistry*, Elsevier, 2005.
13 M. Bernard, C. Baron and A. Deneuville, *Diam Relat Mater*, 2004, **13**, 896–899.
14 L. Niu, J.-Q. Zhu, X. Han, M.-L. Tan, W. Gao and S.-Y. Du, *Phys Lett A*, 2009, **373**, 2494–2500.
15 S. Ernst, L. Aldous and R. G. Compton, *Journal of Electroanalytical Chemistry*, 2011, **663**, 108–112.
16 P. Gan, J. S. Foord and R. G. Compton, *ChemistryOpen*, 2015, **4**, 606–612.
17 S. Sadaf and L. Walder, *Adv Mater Interfaces*, 2017, **4**, 1–10.
18 Y. Hahn and H. Y. Lee, *Arch Pharm Res*, 2004, **27**, 31–34.
19 J. Jacq, *J Electroanal Chem Interfacial Electrochem*, 1971, **29**, 149–180.
20 Q. Li, C. Batchelor-Mcauley, N. S. Lawrence, R. S. Hartshorne and R. G. Compton, *ChemPhysChem*, 2011, **12**, 1255–1257.
21 C. Batchelor-McAuley, Q. Li, S. M. Dapin and R. G. Compton, *Journal of Physical Chemistry B*, 2010, **114**, 4094–4100.
22 C. Batchelor-McAuley, I. B. Dimov, L. Aldous and R. G. Compton, *Proc Natl Acad Sci U S A*, 2011, **108**, 19891–19895.
23 Raymond F. Greene, Jerry M. Collins, Jean F. Jenkins, James L. Speyer and Charles E. Myers, *Cancer Res*, 1983, **43**, 3417–3421.
24 M. J. H. Janssen, D. J. A. Crommelin, G. Storm and A. Hulshoff, *Int J Pharm*, 1985, **23**, 1–11.
25 J. H. Beijnen, O. A. G. J. van der Houwen and W. J. M. Underberg, *Int J Pharm*, 1986, **32**, 123–131.
26 M. J. Wood, W. J. Irwin and D. K. Scott, *J Clin Pharm Ther*, 1990, **15**, 291–300.
27 M. Kelbert, C. S. Pereira, N. A. Daronch, K. Cesca, C. Michels, D. de Oliveira and H. M. Soares, *J Hazard Mater*, 2021, **409**, 124520.
28 R. Jelliffe and M. Neely, in *Individualized Drug Therapy for Patients*, Elsevier, 2017, pp. 383–392.
29 H. C. Ates, J. A. Roberts, J. Lipman, A. E. G. Cass, G. A. Urban and C. Dincer, *Trends Biotechnol*, 2020, **38**, 1262–1277.
30 A. Sparreboom and W. J. Loos, in *Handbook of Anticancer Pharmacokinetics and Pharmacodynamics*, Humana Press, Totowa, NJ, 2004, pp. 169–188.
31 S. Eksborg, H. Ehrsson and B. Ekqvist, *Cancer Chemother Pharmacol*, 1982, **10**, 7–10.
32 M. Yang, Z. Sun, H. Jin and R. Gui, *Microchemical Journal*, 2022, **177**, 107319.

Footnote

† Electronic supplementary information (ESI) available. See DOI: 10.1039/x0xx00000x. ‡Contributed equally.

